

# Changes in Retinal Optical Coherence Tomography Angiography Indexes Over 24 Hours

Barsha Lal, David Alonso-Caneiro, Scott A. Read, Binh Tran, Cong Van Bui, Daniel Tang, Joshua T. Fiedler, Steven Ho, and Andrew Carkeet

School of Optometry & Vision Science, Queensland University of Technology, Kelvin Grove, Brisbane, Australia

Correspondence: Andrew Carkeet, School of Optometry & Vision Science, Queensland University of Technology, Kelvin Grove, Brisbane, QLD-4059, Australia; [a.carkeet@qut.edu.au](mailto:a.carkeet@qut.edu.au).

Received: November 14, 2021

Accepted: March 2, 2022

Published: March 29, 2022

Citation: Lal B, Alonso-Caneiro D, Read SA, et al. Changes in retinal optical coherence tomography angiography indexes over 24 hours. *Invest Ophthalmol Vis Sci.* 2022;63(3):25. <https://doi.org/10.1167/iov.63.3.25>

**PURPOSE.** To evaluate changes in the retinal microvasculature of young adults over 24 hours using optical coherence tomography angiography (OCT-A).

**METHODS.** Participants ( $n = 44$ , mean age  $23.2 \pm 4.1$  years, 24 myopes and 20 nonmyopes) with normal ophthalmological findings were recruited. Two macular OCT-A and OCT scans, systemic blood pressure, intraocular pressure (IOP), and biometry measurements were taken every four hours over 24 hours. Superficial and deep retinal layer en face images were analyzed to extract magnification-corrected vascular indexes using image analysis including foveal avascular zone metrics, vessel density, and perfusion density for the foveal, parafoveal, and perifoveal zones.

**RESULTS.** Significant diurnal variations ( $P < 0.001$ ) were observed in the vessel and perfusion density in the three superficial retinal layer regions, with acrophase between 4:30 PM and 8:30 PM. Only foveal and parafoveal regions of the deep retinal layer exhibited significant diurnal variations with acrophase between 9 AM and 3 PM. Myopes and nonmyopes had different acrophases but not amplitudes in the parafoveal perfusion density of superficial retinal layer ( $P = 0.039$ ). Significant correlations were observed between diurnal amplitudes or acrophases of superficial retinal layer indexes and systemic pulse pressure, IOP, axial length and retinal thickness.

**CONCLUSIONS.** This study shows, for the first time, that significant diurnal variation exists in OCT-A indexes of macular superficial and deep retinal layer over 24 hours and were related to variations in various ocular and systemic measurements. Myopes and nonmyopes showed differences in the timing but not in amplitude of the superficial retinal layer parafoveal perfusion density variations but not in deep retinal layer.

Keywords: diurnal variation, vessel density, perfusion density, 24 hours, OCT-A

Diurnal variation in retinal microvasculature have been relatively unexplored, despite evidence that ocular diurnal variation plays an important role in the regulation of eye growth and pathogenesis of ocular diseases such as glaucoma.<sup>1,2</sup> Optical coherence tomography angiography (OCT-A), a relatively new technique, allows rapid noninvasive imaging of retinal microvasculature at different depths such as the superficial and deep retinal layer and can provide indexes such as vessel and perfusion density that show excellent repeatability.<sup>3-5</sup> The superficial retinal layer is the innermost region and extends from the internal limiting membrane to the inner plexiform layer whereas the deep retinal layer extends from the inner nuclear layer to the outer plexiform layer.<sup>6</sup>

Past studies have explored daytime variations in the OCT-A indexes of superficial and deep retinal layers among healthy participants between 7 AM and 8 PM (Penteado R, et al. *IOVS* 2018;59:ARVO E-Abstract 2856; Rommel F, et al. *IOVS* 2018;59:ARVO E-Abstract 2860).<sup>7-15</sup> Most of these studies did not detect significant variations during the day, except for one study that reported a significant increase ( $P = 0.048$ ) in parafoveal perfusion density between 12 PM and 8 PM

using linear spline model analysis (Penteado R, et al. *IOVS* 2018;59:ARVO E-Abstract 2856). Other ocular measurements also showed significant diurnal variations. Retinal thickness, axial length, and intraocular pressure (IOP) demonstrate a reduction at night whereas choroidal thickness and mean ocular perfusion pressure (MOPP) demonstrate peaks during the night or early morning.<sup>16-18</sup> Additionally, significant fluctuations exists in systemic blood pressure, vascular resistance, and heart rate during nighttime.<sup>19, 20</sup> These ocular and systemic measurements also show significant associations with OCT-A indexes and contribute to the regulation of ocular blood flow.<sup>21-25</sup> Therefore it is expected that retinal OCT-A indexes may also demonstrate significant variations over 24 hours. However, to the best of our knowledge, no previous studies have evaluated OCT-A measurements over a complete 24-hour period. In addition, OCT-A indexes are also affected by axial length and refractive error.<sup>26-28</sup> Myopes had lower superficial and deep vessel/perfusion density and higher vascular resistance index than emmetropes in a number of previous studies.<sup>19, 20, 22, 26-36</sup> However, the role of these factors in diurnal variation of OCT-A indexes over 24 hours is not known.

This study therefore assessed the magnitude and pattern of variation in the microvasculature of superficial and deep retinal layers by capturing a series of macular angiography scans using OCT-A every four hours over 24 hours in young healthy participants. Findings were also compared between myopic and nonmyopic participants. Diurnal variations in axial length, IOP, retinal thickness and systemic blood pressure were also assessed to investigate their relationship with OCT-A indexes. This improved knowledge about diurnal variation will help to establish the expected physiological changes over a 24-hour period in young healthy adults and to assist in the interpretation of clinical changes in OCT-A indexes.

## METHODS

### Participants

This was a prospective observational study conducted among 44 participants including 19 females and 25 males (mean age  $23.2 \pm 4.1$  years, range 18–35 years). Older participants were not included to control for age-related changes in retinal microvasculature.<sup>37–42</sup> Participants with best-corrected vision of 6/7.5 or better, noncycloplegic refraction between  $\pm 6.00$  DS and astigmatism  $\leq 2.00$  DC, normal ophthalmological findings, normal sleep/wake cycle, and good sleep quality (confirmed with the Pittsburgh Sleep Quality Index [PSQI] questionnaire, PSQI score  $\leq 7$ ) were included.<sup>43</sup> Participants were screened a week  $\pm 2$  days before their diurnal measurement session through a detailed medical and ocular history, visual acuity assessment, refraction, slit-lamp examination, IOP measurement, and OCT fundus examination. Noncycloplegic autorefraction (Tomey RC-800; Tomey Corporation, Nayoga, Japan) was done followed by careful subjective refraction with blur back and duochrome technique ensuring relaxed accommodation and aiming for maximum plus to achieve best visual acuity. Participants were asked to refrain from caffeine, alcohol, or tobacco use, vigorous physical activity and abstain from contact lens wear (i.e., to wear spectacles if required) on the experiment day. The Queensland University of Technology Human Research Ethics Committee approved this study and written informed consent was obtained after providing clear explanation of the testing procedures. All participants were treated in accordance with the tenets of the declaration of Helsinki. Participants were classified based upon the subjective, noncycloplegic spherical equivalent refraction (SER) of their right eye as being myopic (SER  $\leq -0.50$ D) or nonmyopic (SER  $> -0.50$ D)<sup>44</sup> and included 24 myopes and 20 nonmyopes. Table 1 summarizes the participants demographic information.

### Data Collection Protocol

For eligible participants, measurements were collected at QUT Optometry Clinic over an approximate 24-hour period

including seven sessions starting around 9 AM and ending around 9 AM the following day. Before each measurement session (excluding 1 AM and 5 AM), 10 minutes wash-out period was provided (watching television at 4 meters) with their habitual spectacles for relaxing accommodation and standardizing the conditions to limit the influence of previous activities upon the measurements. Participants carried out their normal daily activities and were permitted to leave the clinic between 9 AM and 11 PM. They were provided with bedding and remained in the clinic overnight with lights off from 11 PM to 7 AM and were encouraged to sleep. For the measurements at night (1 AM and 5 AM), the room illumination was lowered ( $\sim 2$  Lux) to reduce the impact of measurements on participants' normal circadian rhythm.<sup>45</sup> The following systemic and ocular measurements (only on the right eye) in this order: OCT-A and OCT scans, blood pressure, IOP, and biometry measurements and required 15 to 20 minutes to complete.

### OCT-A and OCT Scanning Protocol and Image Analysis

Two  $3 \text{ mm} \times 3 \text{ mm}$  and  $6 \text{ mm} \times 6 \text{ mm}$  macular angiography enhanced depth imaging scans each were captured through nondilated pupils in dim illumination using Zeiss OCT-A (AngioPlex software, version 11.0; Cirrus HD-OCT 5000; Carl Zeiss Meditec Inc, Dublin, CA, USA) with FastTrac Retinal Tracking.<sup>6</sup> To ensure image quality, the OCT-A images were recaptured if signal strength was  $< 9$  or if they had severe motion artifacts, were not centered on the fovea or exhibited scan tilt  $> 5^\circ$ .<sup>46,47</sup> A larger scan size effectively reduces the image resolution, decreasing the ability to pick up fine capillaries in an image.<sup>48–50</sup> So, the foveal and parafoveal vascular indexes were quantified from  $3 \text{ mm}$  scans for detailed assessment and perifoveal indexes from  $6 \text{ mm}$  scans. The superficial retinal layer (internal limiting membrane to inner plexiform layer) and deep retinal layer (inner nuclear layer to outer plexiform layer) images were exported for extraction of the vascular indexes.

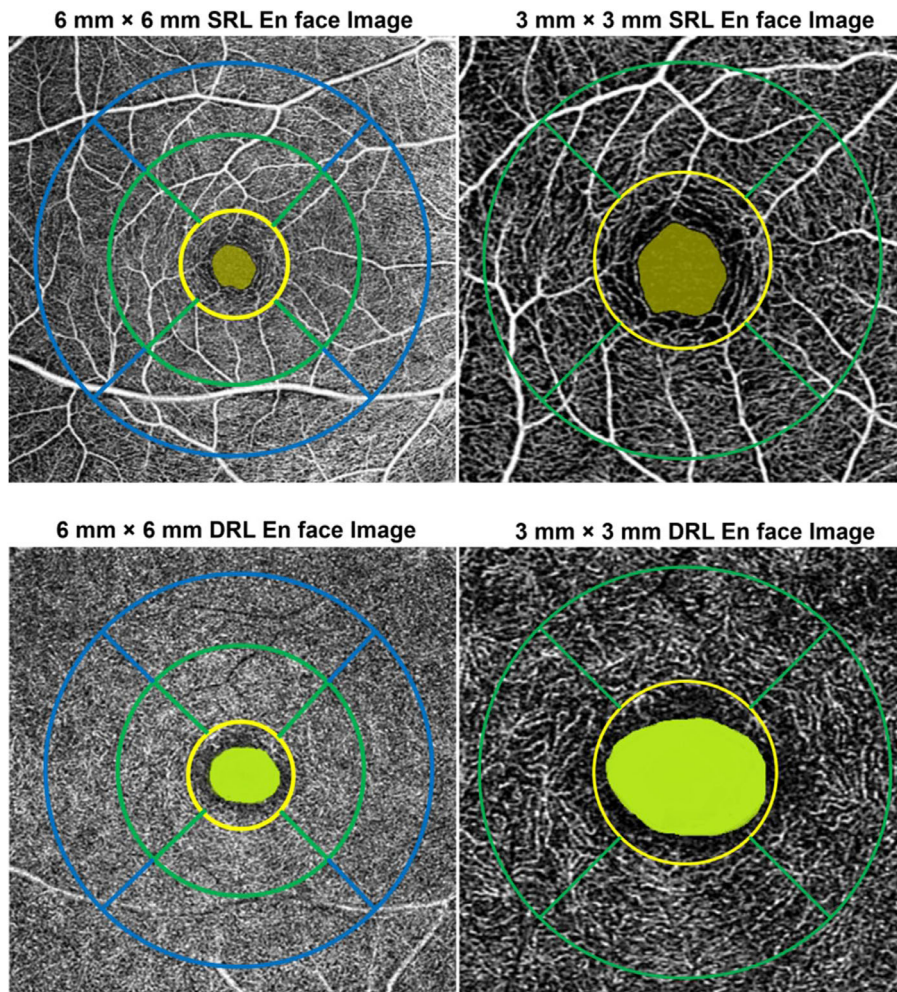
The details of the image analysis and extraction of indexes have been provided in the supplementary section 1. Using a custom image analysis MATLAB program (MathWorks, Natick, MA, USA), the superficial and deep retinal layer images from the seven sessions were registered with each other to ensure that OCT-A indexes were obtained from the same retinal region within the participants. A magnification correction factor determined using a previously described schematic eye method<sup>51</sup> incorporating individual biometry measures (axial length, corneal power, anterior chamber depth and refractive error) was then used to rescale the foveal avascular zone (FAZ) and extract its measurements. Then, the superficial and deep retinal layer images were binarized and skeletonized from which the OCT-A indexes were derived (See Supplementary Section 1). A modified Early Treatment Diabetic Retinopathy Study grid

TABLE 1. Demographics of the Participants

Participants (Female/Male)	Total N = 44 (19/25)	Myopes N = 24 (8/16)	Non-Myopes N = 20 (11/9)
Age (y), mean $\pm$ SD (range)	$23.2 \pm 4.1$ (19.9–35)	$23.5 \pm 4.3$ (19.9–35)	$23.0 \pm 4.0$ (19.9–34.4)
SER (Diopter)	$-1.26 \pm 1.92$ ( $-7.00$ to $1.25$ )	$-2.41 \pm 1.95$ ( $-0.50$ to $-7.00$ )	$0.11 \pm 0.38$ ( $-0.38$ to $+1.25$ )
Astigmatism (Diopter)	$0.40 \pm 0.48$ (0.00 to 2.00)	$0.52 \pm 0.56$ (0.00 to 2.00)	$0.26 \pm 0.32$ (0.00 to 0.75)

SER, spherical equivalent refraction; SD, standard deviation.

Age ( $P = 0.65$ ) and gender distribution ( $P = 0.22$ ) was not significantly different between the two refractive groups.



**FIGURE 1.** Example of the modified early treatment diabetic retinopathy study (ETDRS) grid for the 6 mm × 6 mm (left) and 3 mm × 3 mm (right) superficial retinal layer (SRL) and deep retinal layer (DRL) en face image. Foveal avascular zone: highlighted in green in the center; central/foveal zone (1 mm): inside yellow circle; inner/parafoveal zone (2.5 mm annulus) with quadrants: region between yellow and green circles (left); and outer/perifoveal zone (5 mm annulus) with quadrants: region between green and blue circles (right).

adjusted for magnification<sup>51</sup> which ensured that the indexes between subjects were derived from the same sized retinal regions. The grid was then centered on the images to extract OCT-A indexes from the foveal (central 1 mm), parafoveal (2.5 mm) and perifoveal (5 mm) regions of the superficial and deep retinal layer images (Fig. 1).

The OCT-A indexes extracted from the superficial and deep retinal layers were the FAZ area, FAZ perimeter and the perfusion density and vessel density. The average of the values from the two images captured at each session were taken for analysis. The FAZ area (mm<sup>2</sup>) and FAZ perimeter (mm) were extracted from the superficial and deep retinal layer images of the 3 mm scan as FAZ metrics are not significantly affected by scan size.<sup>48,49</sup> Perfusion density is calculated in percentage as the ratio of image area occupied by the vasculature to the total measured area in the binarized OCT-A image. Perfusion density takes both vessel length and diameter into consideration. Vessel density is calculated in mm/mm<sup>2</sup> as the ratio of the length occupied by the blood vessels to the total measured area in the skeletonized OCT-A image. Vessel density indicates the presence of vessels by quantifying the vessel length density irrespective of the vessel diameters. Large vessels and small capillar-

ies contribute equally to the vessel density quantification.<sup>52</sup> As vessel density has a linear component in it, an additional transverse magnification correction (Equation 1) is required to appropriately adjust the extracted vessel density values for magnification. These corrected values were then used for further analysis.

$$\text{Corrected Vessel density} = \text{Vessel density} / \text{Correction factor} \quad (1)$$

A macular raster enhanced depth imaging-OCT scan was captured twice and analyzed using previously described automated methods in MATLAB to segment different retinal layers (Fig. 2).<sup>53</sup> Magnification corrected total retinal, superficial and deep retinal layer thicknesses of the foveal, parafoveal and perifoveal regions were used for analysis (See Supplementary Section 1).<sup>51</sup>

### Ocular Biometry, IOP and Blood Pressure Measurements

Ocular biometrics including axial length, corneal curvature, and anterior chamber depth were measured using IOL

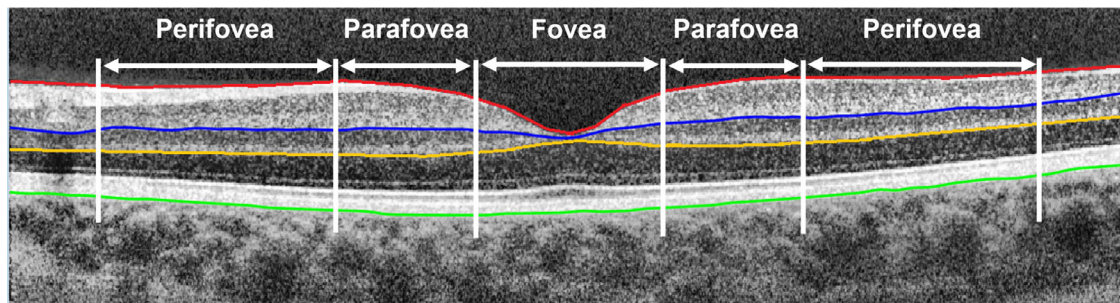


**FIGURE 2.** Example of the segmented boundaries and the analysis zone of a typical OCT image. Segmentation boundaries included internal limiting membrane (red), inner nuclear layer/inner plexiform layer boundary (blue), outer plexiform layer/outer plexiform layer boundary (yellow), and outer boundary of retinal pigment epithelium (green). Total retinal thickness is the axial distance from the retinal pigment epithelium to the inner limiting membrane. Superficial retinal layer thickness is the axial distance from the inner nuclear layer/inner plexiform layer boundary to the inner limiting membrane and deep retinal layer thickness is the axial distance from the inner nuclear layer/inner plexiform layer boundary to the outer plexiform layer/outer plexiform layer boundary. Data were binned into the fovea (1 mm), parafovea (2.5 mm), and perifovea (5 mm).

master (version 5.4; Carl Zeiss, Jena, Germany). A set of five measurements were captured and averaged. Two blood pressure readings including systolic and diastolic blood pressure were taken using an automated sphygmomanometer (version 42NOB; Welch Allyn, Skaneateles Falls, New York, USA) and were averaged for further analysis. IOP was measured using a noncontact tonometer (Canon TX-10 noncontact tonometer; Canon Inc., Tokyo, Japan). An average of three readings of IOP were taken for analysis. The pulse pressure, mean arterial pressure (MAP) and MOPP were calculated for each session from the following equations.<sup>54,55</sup>

$$\text{Pulse Pressure} = \text{SBP} - \text{DBP} \quad (2)$$

$$\text{MAP} = \frac{1}{3} \times (\text{SBP} - \text{DBP}) + \text{DBP} \quad (3)$$

$$\text{MOPP} = \frac{2}{3} \times \text{MAP} - \text{IOP} \quad (4)$$

### Statistical Analysis

Statistical analysis was performed using SPSS (IBM Corp, Armonk, NY, USA), Microsoft Excel, and SigmaPlot (Systat Software, San Jose, CA) software. Repeated measures analysis of variance (ANOVA) was used to investigate the effects of time of day and refractive group for each of the measured parameters along with Bonferroni adjusted pairwise comparison. However, if the amplitudes and acrophase do not show any large within-group variations, a repeated measures ANOVA may not be sensitive enough to detect the diurnal changes and circular statistics can be more appropriate. Using circular statistical tests provides a sensitive test for detecting the occurrence of acrophase and its variation between the groups.<sup>56</sup> Therefore Fourier analysis was conducted to evaluate the acrophase (peak time) and diurnal amplitude for each subject independently.<sup>16,56,57</sup>

The Rayleigh test was used to assess the dispersion of acrophases across the day. Rayleigh's  $r$  values ranges between 0 and 1 with higher values representing more significant clustering of the acrophases indicating significant diurnal variations. The Rayleigh test has been reported to possess very good control of type 1 error rate.<sup>58,59</sup> Mann-Whitney U and Watson's  $U^2$  test were performed to inves-

tigate refractive group differences in diurnal amplitudes and acrophase respectively. Spearman's Rho correlation ( $r_p$ ) and circular correlation ( $r_{cc}$ ) assessed the relationship between amplitude and acrophases of different measurements respectively. The measurements were regarded as in-phase if their acrophases occurred at the same time ( $\pm 2$  hours) and antiphase if their acrophases occurred 12 hours apart ( $\pm 2$  hours).

### RESULTS

Significant diurnal variations were found in a number of the superficial and deep retinal layer OCT-A indexes. Tables 2 and 3 show the daily mean, diurnal amplitudes, diurnal acrophases, Rayleigh test results and repeated measures ANOVA outcomes for the OCT-A indexes of the superficial and deep retinal layers for all participants.

#### Diurnal Variation in the Superficial and Deep Retinal Layer OCT-A Indexes

Significant variations over 24 hours were observed in superficial retinal layer foveal and parafoveal vessel density ( $P = 0.045$  and  $P = 0.005$ , Amplitude:  $0.62 \text{ mm/mm}^2 \pm 0.32$  and  $0.61 \text{ mm/mm}^2 \pm 0.39$ ) and parafoveal and perifoveal perfusion density ( $P = 0.001$  and  $P = 0.037$ , Amplitude:  $1.55\% \pm 0.92$  and  $0.65\% \pm 0.42$ ), respectively. Post hoc analysis with a Bonferroni adjustment revealed that foveal vessel and perfusion density at 5 AM were significantly different from 1 PM ( $P = 0.048$  and  $P = 0.006$ ) and 9 PM ( $P = 0.034$  and  $P = 0.002$ ) and parafoveal perfusion density at 5 AM was significantly different from 1 PM ( $P = 0.04$ ), 5 PM ( $P = 0.01$ ) and 9 PM ( $P = 0.004$ ). The variation in perifoveal perfusion density was no longer significant after Bonferroni adjustment.

The Rayleigh test revealed significant acrophase clustering for vessel and perfusion density in all zones indicating significant diurnal variations across the macular regions. Peak superficial retinal layer vessel and perfusion density were observed between 4:30 PM and 8:30 PM (Table 2) for all the zones. The FAZ area and perimeter at superficial retinal layer did not demonstrate significant variations (all  $P > 0.05$ ).

Repeated measures ANOVA showed significant diurnal variations in vessel and perfusion density for the superficial

**TABLE 2.** Daily Mean, Amplitude, and Acrophase of Diurnal Variation and Its Dispersion, and Time of Day and Refractive Group Comparisons for the OCT-A Indexes in the Foveal, Parafoveal, and Perifoveal Zones of the Superficial and Deep Retinal Layer En Face Images for All Participants

	Daily Mean Mean $\pm$ SEM	Diurnal Amplitude Mean $\pm$ SEM* (%)	Acrophase, Peak Time $\pm$ CD (Hours)	Rayleigh's <i>r</i> , <i>P</i> Value	Time of Day (df = 6, 258) <sup>†</sup>	Time by Refractive Error (df = 6, 252) <sup>†</sup>
SRL-FAZ area (mm <sup>2</sup> )	0.26 $\pm$ 0.01	0.02 $\pm$ 0.01 (7.69%)	10:16 AM $\pm$ 4.66	0.11, >0.09	0.24	0.31
SRL-FAZ perimeter (mm)	2.11 $\pm$ 0.05	0.13 $\pm$ 0.01 (6.16%)	9:48 AM $\pm$ 5.06	0.25, 0.05	0.66	0.66
DRL-FAZ area (mm <sup>2</sup> )	0.68 $\pm$ 0.02	0.08 $\pm$ 0.01 (11.76%)	3:47 PM $\pm$ 4.61	0.42, <0.001 <sup>‡</sup>	0.002 <sup>‡</sup>	0.57
DRL-FAZ perimeter (mm)	3.20 $\pm$ 0.06	0.22 $\pm$ 0.02 (6.88%)	4:14 PM $\pm$ 4.07	0.43, <0.001 <sup>‡</sup>	0.02 <sup>‡</sup>	0.60
SRL-perfusion density (%)						
Fovea	28.13 $\pm$ 0.99	1.68 $\pm$ 0.13 (6.01%)	5:29 PM $\pm$ 4.68	0.26, 0.05 <sup>‡</sup>	0.33	0.38
Parafovea	48.62 $\pm$ 0.26	1.55 $\pm$ 0.14 (3.19%)	6:13 PM $\pm$ 3.98	0.46, <0.001 <sup>‡</sup>	0.001 <sup>‡</sup>	0.04 <sup>‡</sup>
Perifovea	34.98 $\pm$ 0.11	0.65 $\pm$ 0.06 (1.85%)	6:55 PM $\pm$ 3.90	0.48, <0.001 <sup>‡</sup>	0.004 <sup>‡</sup>	0.73
SRL-vessel density (mm/mm <sup>2</sup> )						
Fovea	8.15 $\pm$ 0.28	0.61 $\pm$ 0.05 (7.59%)	4:50 PM $\pm$ 4.55	0.48, <0.001 <sup>‡</sup>	0.045 <sup>‡</sup>	0.42
Parafovea	14.35 $\pm$ 0.15	0.60 $\pm$ 0.06 (4.45%)	5:53 PM $\pm$ 4.13	0.41, <0.001 <sup>‡</sup>	0.005 <sup>‡</sup>	0.82
Perifovea	14.15 $\pm$ 0.01	0.46 $\pm$ 0.04 (3.29%)	7:13 PM $\pm$ 4.57	0.28, 0.04 <sup>‡</sup>	0.20	0.64
DRL-perfusion density (%)						
Fovea	20.92 $\pm$ 0.95	3.88 $\pm$ 0.43 (18.55%)	2:58 PM $\pm$ 4.68	0.26, 0.05 <sup>‡</sup>	0.005 <sup>‡</sup>	0.65
Parafovea	50.05 $\pm$ 0.55	1.92 $\pm$ 0.15 (3.83%)	11:17 PM $\pm$ 4.54	0.29, 0.03 <sup>‡</sup>	0.08	0.67
Perifovea	38.72 $\pm$ 0.48	0.54 $\pm$ 0.05 (1.39%)	9:27 PM $\pm$ 5.17	0.08, >0.9	0.91	0.76
DRL-vessel density (mm/mm <sup>2</sup> )						
Fovea	7.16 $\pm$ 0.29	1.14 $\pm$ 0.12 (16.24%)	2:28 PM $\pm$ 4.64	0.27, 0.045 <sup>‡</sup>	0.002 <sup>‡</sup>	0.53
Parafovea	13.74 $\pm$ 0.19	0.67 $\pm$ 0.05 (4.92%)	9:29 PM $\pm$ 4.49	0.31, 0.01 <sup>‡</sup>	0.09	0.72
Perifovea	16.73 $\pm$ 0.21	0.37 $\pm$ 0.04 (2.24%)	10:24 PM $\pm$ 5.13	0.10, 0.67	0.54	0.76

SEM, standard error of mean; CD, circular deviation; SRL, superficial retinal layer; DRL, deep retinal layer.

\* Diurnal amplitude expressed as the percentage of the daily mean value.

<sup>†</sup> *P* values from repeated measures ANOVA for time of day, and time of day by refractive error.

<sup>‡</sup> *P* < 0.05.

retinal layer parafoveal quadrants except superior whereas only perifoveal superior and nasal perfusion density showed significant results (Table 3). However, significant clustering of acrophase in the perfusion density of parafoveal and perifoveal quadrants and vessel density of the parafoveal quadrants were observed (Rayleigh's *r*, *P* < 0.05 for all).

Only foveal vessel and perfusion density of the deep retinal layer exhibited significant diurnal variations between the sessions (*P* = 0.005 and *P* = 0.002) which was no longer significant after Bonferroni adjustment. However, both deep retinal layer foveal and parafoveal vessel and perfusion density showed clustering of acrophase (Table 2) indicating significant diurnal variations. The deep retinal layer parafoveal vessel density and perfusion density peaks were observed between 9 PM and 11:30 PM and earlier in the mid-afternoon for the foveal zone. The FAZ area and perimeter at deep retinal layer showed significant diurnal variation (time of day effect, *P* = 0.002 and 0.019 and Rayleigh's *r* = 0.42 and 0.43, *P* < 0.001) with acrophase at 3:47 PM and 4:14 PM. Post hoc analysis revealed significant differences between FAZ measurements at 1 PM and 1 AM and between measurements at 9 PM and 9 AM (*P* < 0.05 for all). Only the perfusion density of the superior parafoveal zone demonstrated significant diurnal variations (*P* = 0.026), whereas the perifoveal quadrants did not exhibit significant variations.

### Time by Refractive Groups Interaction in the Superficial and Deep Retinal Layer OCT-A Indexes

Myopes and nonmyopes showed different pattern of variation in the superficial retinal layer parafoveal perfusion density i.e., a significant time of day by refractive group interaction (*P* = 0.04). Further analysis showed a significant difference (*P* = 0.02) in the acrophase of superficial retinal layer parafoveal perfusion density between myopes (5:10 PM  $\pm$  3.31 hours) and nonmyopes (8:57 PM  $\pm$  4.36 hours). Figure 3 demonstrates the mean changes in superficial

retinal layer parafoveal vessel and perfusion density changes over 24 hours for the two refractive groups. Figure 4 depicts polar diagrams for parafoveal vessel and perfusion density of superficial retinal layer plotting acrophase against amplitude for individual myopes and nonmyopes. A significant time of day by refractive group interaction (*P* = 0.04) was found in the parafoveal nasal perfusion density with a significant difference in acrophase of superficial retinal layer nasal perfusion density (*P* = 0.02) between myopes (4:54 PM  $\pm$  3.26 hours) and nonmyopes (8:35 PM  $\pm$  4.50 hours).

None of the indexes for either of the layers showed any significant difference (all *P* > 0.05) in diurnal amplitude between the two refractive groups for any of the considered zones. The daily mean vessel density (mm/mm<sup>2</sup>) in the parafoveal and perifoveal zones of the superficial retinal layer (Myopes: 13.32  $\pm$  0.92 and 13.86  $\pm$  0.80; Nonmyopes: 14.08  $\pm$  0.76 and 14.94  $\pm$  0.92) and deep retinal layer (Myopes: 13.37  $\pm$  1.39 and 14.18  $\pm$  0.98; Nonmyopes: 16.12  $\pm$  0.76 and 17.46  $\pm$  1.52) were significantly greater in the nonmyopes (*P* < 0.05 for all). Similar results were also noted in the daily mean vessel density of all the perifoveal and parafoveal quadrants (*P* < 0.05 for all). The remaining indexes in each of the layers and zones did not show any significant refractive group effects (*P* > 0.05 for all).

### Diurnal Rhythm in Ocular and Systemic Measurements

Axial length, total retinal, superficial, and deep retinal layer thicknesses, IOP, MAP, pulse pressure and MOPP all demonstrated significant diurnal variations (Table 4). The total retinal and superficial retinal layer thickness exhibited significant time of day effects and time by refractive group interactions at the parafovea and perifovea respectively whereas deep retinal layer thickness demonstrated time of day effects only at parafovea and perifovea. A significant effect of refractive group was only noted in axial length,

**TABLE 3.** Amplitude of Diurnal Variation, Acrophase of Diurnal Variation and its Dispersion, and Time of Day and Refractive Group Comparisons for Vessel and Perfusion Density in the Parafoveal and Perifoveal Zone Quadrants of the Superficial and Deep Retinal Layer En Face Images for all Participants

	Diurnal Amplitude Mean $\pm$ SEM	Acrophase, Peak Time $\pm$ CD (Hours)	Rayleigh's $r$ , $P$ Value	Time of Day (df = 6, 258)*	Time by Refractive Error (df = 6, 252)*
SRL-perfusion density (%)					
Parafovea-superior	2.21 $\pm$ 0.20	7:27 PM $\pm$ 4.59	0.28, 0.04 <sup>†</sup>	0.13	0.51
Parafovea-nasal	1.65 $\pm$ 0.16	6:55 PM $\pm$ 4.31	0.36, 0.001 <sup>†</sup>	0.01 <sup>†</sup>	0.04 <sup>†</sup>
Parafovea-inferior	2.09 $\pm$ 0.19	4:23 PM $\pm$ 3.89	0.48, <0.001 <sup>†</sup>	0.001 <sup>†</sup>	0.93
Parafovea-temporal	1.68 $\pm$ 0.0.13	6:16 PM $\pm$ 4.16	0.41, <0.001 <sup>†</sup>	0.003 <sup>†</sup>	0.36
Perifovea-superior	0.98 $\pm$ 0.10	8:22 PM $\pm$ 4.30	0.37, 0.001 <sup>†</sup>	0.02 <sup>†</sup>	0.43
Perifovea-nasal	0.90 $\pm$ 0.07	5:52 PM $\pm$ 4.31	0.36, 0.001 <sup>†</sup>	0.05 <sup>†</sup>	0.38
Perifovea-inferior	0.91 $\pm$ 0.7	6:19 PM $\pm$ 4.49	0.31, 0.01 <sup>†</sup>	0.24	0.96
Perifovea-temporal	0.83 $\pm$ 0.09	6:33 PM $\pm$ 4.09	0.43, <0.001 <sup>†</sup>	0.08	0.55
SRL-vessel density (mm/mm <sup>2</sup> )					
parafovea-superior	0.80 $\pm$ 0.08	6:57 PM $\pm$ 4.69	0.26, 0.05 <sup>†</sup>	0.18	0.91
parafovea-nasal	0.65 $\pm$ 0.06	5:48 PM $\pm$ 4.36	0.35, 0.002 <sup>†</sup>	0.05 <sup>†</sup>	0.19
parafovea-inferior	0.73 $\pm$ 0.06	5:02 PM $\pm$ 3.79	0.26, 0.03 <sup>†</sup>	0.001 <sup>†</sup>	0.95
parafovea-temporal	0.65 $\pm$ 0.06	6:26 PM $\pm$ 4.32	0.36, 0.001 <sup>†</sup>	0.01 <sup>†</sup>	0.65
perifovea-superior	0.65 $\pm$ 0.06	8:26 PM $\pm$ 4.83	0.20, 0.14	0.10	0.34
perifovea-nasal	0.63 $\pm$ 0.05	6:40 PM $\pm$ 4.69	0.25, 0.06	0.47	0.65
perifovea-inferior	0.61 $\pm$ 0.05	6:56 PM $\pm$ 4.69	0.24, 0.06	0.56	0.61
perifovea-temporal	0.57 $\pm$ 0.06	8:43 PM $\pm$ 4.75	0.23, 0.09	0.75	0.35
DRL-perfusion density (%)					
Parafovea-superior	3.08 $\pm$ 0.28	7:49 PM $\pm$ 4.51	0.30, 0.01 <sup>†</sup>	0.07	0.12
Parafovea-nasal	3.07 $\pm$ 0.29	11:41 PM $\pm$ 4.15	0.41, <0.001 <sup>†</sup>	0.03 <sup>†</sup>	0.82
Parafovea-inferior	3.70 $\pm$ 0.34	2:55 AM $\pm$ 5.20	0.07, <0.9	0.71	0.68
Parafovea-temporal	2.84 $\pm$ 0.24	1:46 AM $\pm$ 4.99	0.15, 0.36	0.13	0.51
Perifovea-superior	0.71 $\pm$ 0.06	2:02 AM $\pm$ 4.87	0.19, 0.20	0.24	0.72
Perifovea-nasal	0.84 $\pm$ 0.08	6:29 PM $\pm$ 5.15	0.09, >0.90	0.86	0.89
Perifovea-inferior	0.76 $\pm$ 0.08	7:59 AM $\pm$ 5.12	0.10, 0.67	0.69	0.18
Perifovea-temporal	0.71 $\pm$ 0.07	6:29 PM $\pm$ 5.11	0.11, 0.61	0.33	0.79
DRL-vessel density (mm/mm <sup>2</sup> )					
Parafovea-superior	0.99 $\pm$ 0.09	7:49 PM $\pm$ 4.46	0.32, 0.005 <sup>†</sup>	0.04 <sup>†</sup>	0.41
Parafovea-nasal	0.99 $\pm$ 0.08	10:18 PM $\pm$ 4.38	0.34, 0.004 <sup>†</sup>	0.08	0.79
Parafovea-inferior	0.98 $\pm$ 0.09	7:44 PM $\pm$ 5.10	0.11, 0.61	0.43	0.77
Parafovea-temporal	0.89 $\pm$ 0.08	10:29 PM $\pm$ 5.09	0.11, 0.61	0.10	0.44
Perifovea-superior	0.49 $\pm$ 0.04	11:23 PM $\pm$ 4.65	0.25, 0.06	0.07	0.89
Perifovea-nasal	0.57 $\pm$ 0.06	4:34 PM $\pm$ 4.84	0.20, 0.14	0.60	0.37
Perifovea-inferior	0.51 $\pm$ 0.05	5:38 AM $\pm$ 5.24	0.06, >0.9	0.76	0.27
Perifovea-temporal	0.48 $\pm$ 0.05	2:10 AM $\pm$ 5.38	0.01, >0.9	0.34	0.53

SEM, Standard Error of Mean; CD, Circular Deviation; df, degree of freedom; SRL, superficial retinal layer; DRL, deep retinal layer.

\*  $P$  values from repeated measures ANOVA for time of day and time of day by refractive error.

<sup>†</sup>  $P < 0.05$ .

due to the well-documented longer axial length associated with myopia.

### Relationships of the Superficial and Deep Retinal Layer OCT-A Indices Diurnal Rhythm

The diurnal amplitude of the superficial retinal layer perfusion density was negatively correlated with the parafoveal retinal thickness ( $r_p = -0.30$ ,  $P = 0.046$ ) and MOPP diurnal amplitudes ( $r_p = -0.44$ ,  $P = 0.003$ ). The diurnal amplitudes of superficial retinal layer foveal vessel density and perfusion density were weakly correlated with the diurnal amplitudes of pulse pressure ( $r_p = -0.39$ ,  $P = 0.0093$  and  $r_p = -0.36$ ,  $P = 0.02$ ) and IOP ( $r_p = -0.37$ ,  $P = 0.02$  and  $r_p = -0.39$ ,  $P = 0.010$ ). The deep retinal layer perfusion density diurnal amplitude showed significant correlation with parafoveal deep retinal layer thickness and total retinal thickness amplitudes ( $r_p = 0.40$ ,  $P = 0.007$  and  $r_p = -0.45$ ,  $P = 0.002$ ). The

deep retinal layer parafoveal vessel density and perfusion density and axial length amplitudes were also correlated ( $r_p = 0.33$ ,  $P = 0.03$  and  $r_p = 0.49$ ,  $P = 0.001$ ).

The acrophases of superficial retinal layer perfusion density and thickness at parafovea were also negatively correlated ( $r_{cc} = -0.34$ ,  $P = 0.01$ ) (Fig. 5). The acrophases of superficial retinal layer perfusion and vessel density at parafovea were significantly correlated with the acrophases of IOP ( $r_{cc} = 0.40$ ,  $P = 0.001$  and  $r_{cc} = 0.42$ ,  $P < 0.001$ ) and pulse pressure ( $r_{cc} = 0.31$ ,  $P = 0.04$  for both) (Fig. 6). The IOP and FAZ metrics of deep retinal layer acrophases were also correlated ( $r_{cc} = 0.45$ ,  $P < 0.001$  and  $r_{cc} = 0.42$ ,  $P < 0.001$ ).

### DISCUSSION

This is the first study to evaluate the pattern and magnitude of diurnal variation in the retinal microvasculature

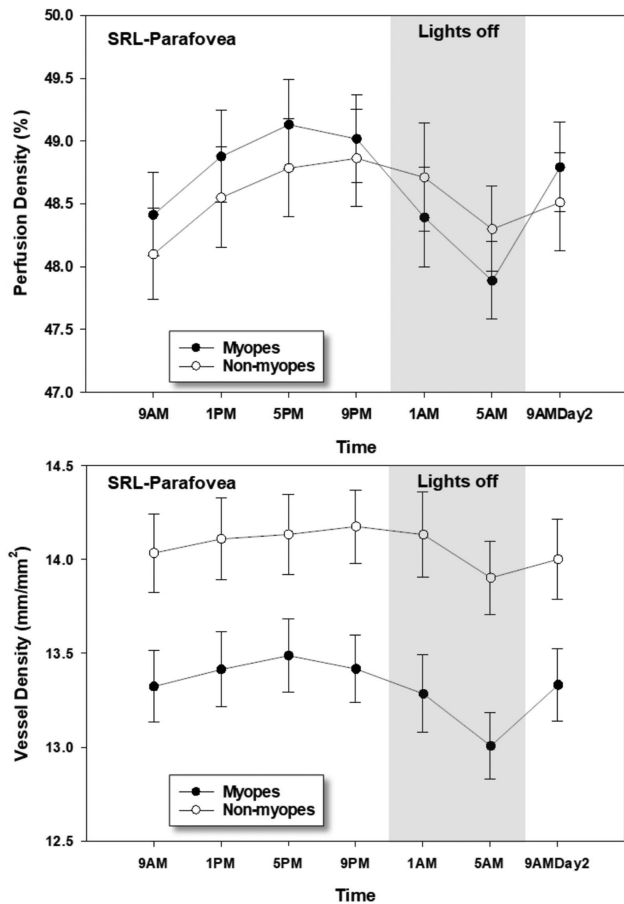


**FIGURE 3.** Perfusion density (top) and vessel density (bottom) of the superficial retinal layer (SRL) at parafovea in myopes and nonmyopes plotted across 24 hours. The error bars represent one standard error of the mean. Significant changes over 24 hours were found ( $P < 0.05$ ) for both parafoveal superficial retinal layer vessel and perfusion density. Both indexes were lowest at 5 AM for the two refractive groups. A significant time by refractive group interaction ( $P = 0.04$ ) was observed only for parafoveal perfusion density.

over a full 24-hour period using OCT-A with comparisons between myopes and nonmyopes. Perfusion and vessel density demonstrated significant diurnal variations in the foveal, parafoveal, and perifoveal zones of the superficial and deep retinal layers, with their peaks between afternoon and late evening and troughs during the night and early morning hours except for perifoveal deep retinal layer vessel and perfusion density, which did not show significant change. The diurnal pattern or amplitude of the OCT-A indexes were also found to be correlated with changes in retinal thickness, axial length, IOP and pulse pressure. Furthermore, the findings showed significant differences in the timing of the diurnal rhythms of superficial retinal layer indexes at the parafovea between myopic and nonmyopic healthy adults but the diurnal rhythms in the foveal and perifoveal zones or the deep retinal layer indexes were not different between refractive groups.

A change in retinal blood flow over 24 hours could potentially cause a corresponding change in the detectability of fine capillaries by the OCT-A imaging method. This will eventually result in variation in the OCT-A indexes. Studies in the past have evaluated OCT-A variations using

different protocols with measurements captured between 7 AM and 8 PM in the superficial and deep retinal layers among healthy adults (Penteado R, et al. *IOVS* 2018;59:ARVO E-Abstract 2856; Rommel F, et al. *IOVS* 2018;59:ARVO E-Abstract 2860).<sup>7-15</sup> We hypothesized that ocular blood flow may be different at night compared to day,<sup>60</sup> so the present study recruited young healthy participants and captured measurements over 24 hours encompassing seven measurement points. This allowed a more comprehensive understanding of the normal diurnal variation in the macular microvasculature.

The diurnal variation of the superficial retinal layer perfusion and vessel density in the foveal and parafoveal regions showed similar trends, with measurements highest in late afternoon and lowest during sleeping hours. Most previous studies found insignificant daily fluctuations in superficial retinal layer OCT-A indexes between 7 AM to 8 PM (Rommel F, et al. *IOVS* 2018;59:ARVO E-Abstract 2860).<sup>7-15</sup> In the present study, most changes occurred during night between 9 PM to 5 AM with very small changes taking place between 9 AM and 9 PM. Only one previous study found a small but significant increase in the parafoveal region perfusion density between 12 PM and 8 PM, however the layer was not specified (Penteado R, et al. *IOVS* 2018;59:ARVO E-Abstract 2856). A small number of studies evaluated variations in deep retinal layer OCT-A indexes between 8 AM to 8 PM among healthy adults and reported them to be stable throughout the day.<sup>8,10,11,15</sup> Blood flow in the deep retinal layer might be expected to increase at night, since it is nearest to the photoreceptors layer and supplies for its increased metabolic demands in the dark. Nesper et al.<sup>61</sup> found a significant transient increase in superficial retinal layer and decrease in deep retinal layer perfusion density during the transition from dark to light. However, the current study observed lowest deep indexes in the foveal region during the sleeping hours (2 AM and 3 AM) and in the parafoveal region during late morning (9 AM and 11:30 AM). The deep retinal layer is supplied by the vertical anastomoses from the superficial vascular plexus whereas the superficial retinal layer is directly supplied by the central retina artery.<sup>24</sup> The capillary flow between the superficial and deep network happens through the anatomical capillary interconnections. This interconnection between these two capillary networks could explain the different physiological variations taking place in these layers.<sup>24,62,63</sup>

In the current study, the diurnal amplitudes of superficial and deep retinal layer perfusion density and of total retinal thickness at the parafovea were negatively correlated, but not their acrophase. This is in contrast with the finding reported by Milani et al.<sup>12</sup> where the parafoveal superficial retinal layer perfusion density and retinal thickness diurnal changes during the day showed a weak positive correlation. However, that study included healthy participants and those with glaucoma and ocular hypertension, and only two time points (morning and evening) were assessed. Though the reason is not clear, it is likely that changes in the outer retinal layers occurring over 24 hours may have contributed towards the relationship.<sup>17</sup> In addition, the vessel and perfusion density variations (acrophase for superficial retinal layer: 5:29 PM and 4:50 PM; acrophase for deep retinal layer: 2:58 PM and 2:28 PM) were in-phase with total retinal thickness in the foveal region (acrophase: 3:44 PM). Retinal perfusion and thickness have also been more highly correlated in the foveal region than parafoveal region in the previous cross-sectional studies.<sup>29,64-66</sup>

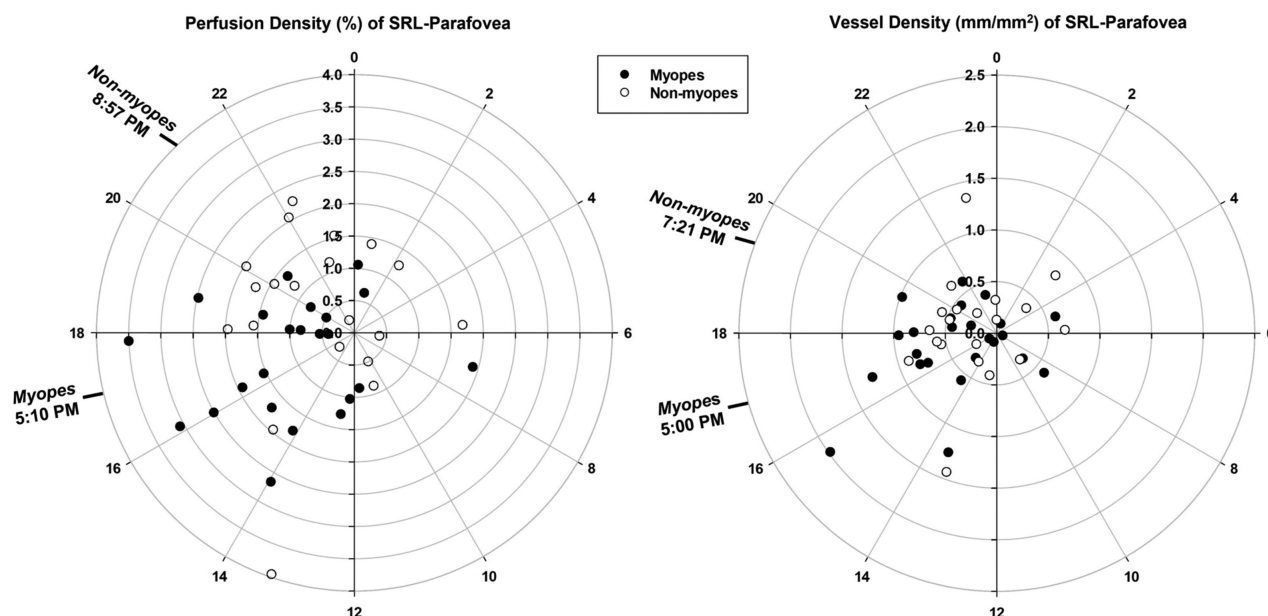


**FIGURE 4.** Diurnal amplitude of change (distances from center) plotted against acrophase time (around the perimeter, 24-hour clock) for myopes and nonmyopes for superficial retinal layer (SRL) vessel density (right) and perfusion density (left). Mean acrophase for myopes and nonmyopes are indicated by the time in bold. The acrophase of superficial retinal layer parafoveal perfusion density in myopes was significantly ( $P = 0.02$ ) earlier than nonmyopes whereas the vessel density acrophase difference did not reach statistical significance.

**TABLE 4.** Amplitude of Diurnal Variation, Acrophase of Diurnal Variation and Its Dispersion, and Time of Day and Refractive Group Comparisons for Ocular and Systemic Measurements for All Participants

	<b>Diurnal Amplitude Mean ± SEM</b>	<b>Acrophase,Peak Time ± CD (Hours)</b>	<b>Rayleigh's <i>r</i>, P Value</b>	<b>Time of Day (df = 6, 258)*</b>	<b>Time by Refractive Error (df = 6, 252) *</b>
Axial Length (mm)	0.04 ± 0.01	2:14 PM ± 3.17	0.65, <0.001†	<0.001†	0.32
Total Retinal Thickness (µm)					
Fovea	5.89 ± 0.36	3:44 PM ± 2.08	0.85, <0.001†	<0.001†	0.84
Parafovea	3.39 ± 0.33	1:14 PM ± 4.40	0.34, 0.003†	0.001†	0.69
Perifovea	3.57 ± 0.60	5:02 AM ± 4.58	0.28, 0.04†	0.02†	0.04†
SRL Thickness (µm)					
Fovea	4.02 ± 0.31	6:24 AM ± 5.19	0.08, 0.900	0.77	0.50
Parafovea	2.46 ± 0.21	4:05 AM ± 4.19	0.40, <0.001†	<0.001†	<0.001†
Perifovea	2.87 ± 0.30	2:50 AM ± 4.86	0.19, 0.20	0.12	0.34
DRL Thickness (µm)					
Fovea	4.95 ± 0.47	11:28 AM ± 5.07	0.12, 0.65	0.44	0.66
Parafovea	4.93 ± 0.58	12:31 PM ± 4.59	0.28, 0.04†	0.04†	0.47
Perifovea	2.59 ± 0.36	5:40 AM ± 3.82	0.50, <0.001†	0.05†	0.53
Pulse Pressure (mm Hg)	7.04 ± 0.75	5:57 PM ± 4.10	0.42, <0.001†	0.05†	0.78
Mean arterial pressure(mm Hg)	7.68 ± 0.63	11:50 PM ± 4.25	0.38, <0.001†	0.004†	0.60
IOP (mm Hg)	3.81 ± 0.29	12:13 PM ± 2.98	0.69, <0.001†	<0.001†	0.74
MOPP (mm Hg)	6.77 ± 0.54	11:59 PM ± 3.15	0.66, <0.001†	<0.001†	0.86

SEM, standard error of mean; CD, circular deviation; df, degree of freedom; SRL, superficial retinal layer; DRL, deep retinal layer.

\* P values from repeated measures ANOVA for time of day, and time of day by refractive error.

†  $P < 0.05$ .

This study also, reports for the first time, significant diurnal variation in the parafoveal superficial and deep retinal layers thickness over 24 hours and evaluates their relationship with OCT-A indexes variations. The photoreceptor's metabolic demands are known to affect retinal vasculature under normal physiological conditions.<sup>67</sup> At night, usually the photoreceptor outer segment + RPE layer is thickest whereas photoreceptor inner segment is thinnest

when evaluated over 24 hours<sup>17</sup> corresponding to the changes observed in superficial and deep retinal layer thickness respectively in the present study. We speculate that these similarities between the variations of different retinal layers might suggest a possible interaction between the physiological variations of retinal thickness and perfusion. The presence of diurnal changes in the retinal perfusion could also be related to the metabolic demands of the inner



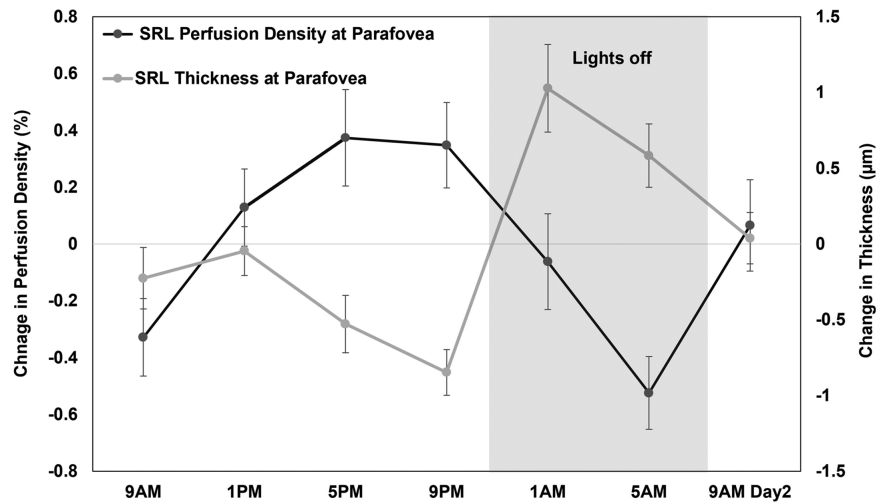


FIGURE 5. Mean ( $\pm 1$  standard error of the mean) change in perfusion density (*black*) and thickness (*gray*) of superficial retinal layer (SRL) in the parafoveal region across 24 hours demonstrating their variations in approximately antiphase with each other and their acrophases were significantly correlated ( $r_{cc} = -0.34$ ,  $P = 0.01$ ).

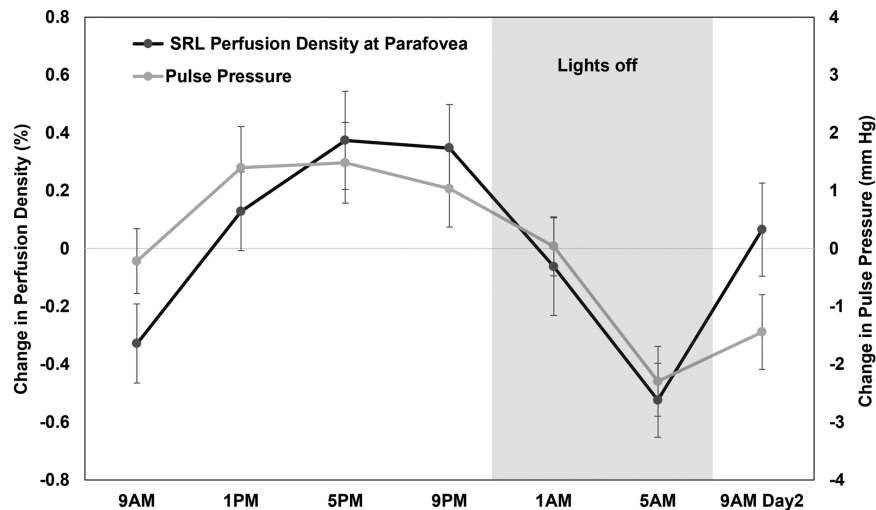


FIGURE 6. Mean ( $\pm 1$  standard error of the mean) change in perfusion density (*black*) of superficial retinal layer (SRL) in the parafoveal region and pulse pressure (*gray*) across 24 hours demonstrating their variations in phase with each other and their acrophases were significantly correlated ( $r_{cc} = 0.31$ ,  $P = 0.04$ ).

retinal cells or the presence of autonomous inner retinal clocks that regulate dopamine release and influence retinal perfusion.<sup>68–70</sup>

The superficial and deep retinal layer perfusion and vessel density variations (acrophase for superficial retinal layer: 6:13 PM and 5:53 PM; acrophase for deep retinal layer: 11:17 PM and 9:29 PM) were approximately antiphase to the superficial retinal layer thickness (acrophase: 4:05 AM) and deep retinal layer thickness (acrophase: 12:31 PM) variations in parafovea, respectively (Fig. 5). The mechanism behind this antiphase relationship is unclear, although we speculate that the thickness of the outer and inner segments of the photoreceptors at night might inversely affect the perfusion of the inner retinal layer's perfusion. Macular perfusion has been reported to significantly correlate with superficial retinal layer thickness.<sup>71</sup>

Systemic assessment of the blood flow dynamics in the nocturnal and morning hours has been strongly emphasized in the literature owing to its association with abnormal cardiovascular events.<sup>72</sup> It has been reported that retinal perfusion/blood flow is sensitive toward vascular factors such as MAP, pulse pressure and MOPP.<sup>73,74</sup> Both MAP and pulse pressure showed significant diurnal variation with lowest readings around midday and early morning making pulse pressure approximately in-phase with superficial retinal layer perfusion and vessel density (Fig. 6). In addition, their diurnal amplitudes and acrophases were weakly correlated. This could be theoretically explained by high vascular resistance during morning, in turn increasing diastolic blood pressure and reducing pulse pressure and blood flow during the early hours.<sup>19,20</sup> The current study also involved postural changes from supine to standing followed by sitting and

no adaptation time was provided to adapt to these postural changes before the night OCT-A scans were taken. It has been recommended to wait about one to five minutes for measuring the maximum effect of posture change.<sup>75–78</sup> So, the effect of supine posture on the current study measurements of ocular blood flow at night cannot be completely ruled out.<sup>79–81</sup>

Axial length changes can result in subtle microstructural retinal changes especially in high myopia.<sup>26,82,83</sup> Previous studies have shown positive correlation between deep retinal layer perfusion density and axial length. The diurnal amplitudes of the deep parafoveal vessel and perfusion density and axial length were positively correlated, and their variations were in-phase with each other (peaks between 2 PM and 3 PM) in the present study. In addition, myopes also showed significantly lower mean vessel density across the day in the parafoveal and perifoveal zones of both the layers than nonmyopes. Diurnal fluctuations in IOP and MOPP and their acrophases were also significantly correlated to that of superficial retinal layer vessel and perfusion density in this study considering that MOPP plays an integral role in regulating blood flow in the retina<sup>25</sup> and is also affected by posture change.<sup>81</sup> Baek et al.<sup>14</sup> also found that the diurnal change in macular OCT-A indexes were associated with MOPP changes.

Myopes and nonmyopes showed significantly different patterns of variation over 24 hours for superficial retinal layer perfusion density of the parafovea with the acrophase occurring 4-hours earlier in myopes. This may arise due to the differences between myopes and nonmyopes in terms of ocular blood flow. For instance, a number of studies<sup>84–86</sup> showed increased vascular resistance index and decreased pulsatile ocular blood flow with increasing myopia or axial length. Considering that vascular resistance index is already high among myopes compared to nonmyopes, it further increases during the morning<sup>20</sup> resulting in more myopes demonstrating their trough in OCT-A indexes in the morning. However, the present study did not find any difference in the variation pattern in axial length and systemic parameters between myopes and nonmyopes. It may be that local retinal vascular dynamics varied between the refractive groups. Though the retinal blood flow is autoregulated, Kur et al.<sup>87</sup> reported local regulation of retinal blood flow in response to flickering light.

Though the diurnal changes observed are of relatively small magnitude, the current result provides normative data for OCT-A diurnal amplitude of vascular indexes over 24 hours. When expressed in terms of percentage of the daily mean, the diurnal amplitude ranged between 1.85% to 18.55% in different zones of the two layers. These results can serve as a baseline of expected change when analyzing the diurnal variation over 24 hours in conditions such as glaucoma and hypertension. The diurnal changes of OCT-A indexes were more marked in the parafoveal region and were significantly related to the ocular and systemic parameters, similar to the findings in patients with glaucoma.<sup>10</sup> Though Bonferroni adjusted comparisons were conducted to reduce the chance of type 1 errors within each of the individual ANOVA comparing seven sessions, the use of multiple repeated measures ANOVA analysis for different Early Treatment Diabetic Retinopathy Study regions and layers might also increase the chances of type 1 errors. Replication of 24-hour diurnal variation studies in retinal microvasculature is warranted for more definitive conclusions. Our results might also be affected by the “first night effect” caus-

ing altered sleep due to participants sleeping in a new environment.<sup>88</sup> It should be noted that our results are confined to young healthy adults and might not apply to children due to their ongoing refractive development or to older adults due to age-related vascular changes.<sup>89,90</sup> Further studies are required to profile complete diurnal variation over 24 hours across age groups and ocular vascular diseases.

In conclusion, this study for the first time demonstrates that significant diurnal variation over 24 hours exists in OCT-A indexes of macular retinal microvasculature including superficial and deep retinal layer in healthy young adults. Myopes and nonmyopes showed variation only in the diurnal pattern of the parafoveal superficial retinal layer perfusion density but not in diurnal amplitude. The diurnal variation in the deep retinal layer indexes did not demonstrate any difference between the two refractive groups. The diurnal pattern and amplitude of the OCT-A indexes were found to be correlated with ocular and systemic measurements.

### Acknowledgments

Disclosure: **B. Lal**, None; **D. Alonso-Caneiro**, None; **S.A. Read**, None; **B. Tran**, None; **C. Van Bui**, None; **D. Tang**, None; **J.T. Fiedler**, None; **S. Ho**, None; **A. Carkeet**, None

### References

1. Chakraborty R, Ostrin LA, Nickla DL, Iuvone PM, Pardue MT, Stone RA. Circadian rhythms, refractive development, and myopia. *Ophthalm Physiol Opt*. 2018;38:217–245.
2. Asrani S, Zeimer R, Wilensky J, Gieser D, Vitale S, Lindemuth K. Large diurnal fluctuations in intraocular pressure are an independent risk factor in patients with glaucoma. *J Glaucoma*. 2000;9:134–142.
3. Linderman RE, Muthiah MN, Omoba SB, et al. Variability of foveal avascular zone metrics derived from optical coherence tomography angiography images. *Transl Vis Sci Technol*. 2018;7(5):20.
4. Chen FK, Menghini M, Hansen A, Mackey DA, Constable IJ, Sampson DM. Intrasession repeatability and interocular symmetry of foveal avascular zone and retinal vessel density in OCT angiography. *Transl Vis Sci Technol*. 2018;7(1):6.
5. Zhao Q, Yang WL, Wang XN, et al. Repeatability and reproducibility of quantitative assessment of the retinal microvasculature using optical coherence tomography angiography based on optical microangiography. *Biomed Environ Sci*. 2018;31:407–412.
6. Rosenfeld PJ, Durbin MK, Roisman L, et al. ZEISS angioplex spectral domain optical coherence tomography angiography: technical aspects. *Dev Ophthalmol*. 2016;56:18–29.
7. Wu JH, Penteado RC, Moghimi S, Zangwill LM, Proudfoot JA, Weinreb RN. Diurnal variation of retinal vessel density in healthy human eyes. *J Glaucoma*. 2021;30:820–826.
8. Milani P, Urbini LE, Bulone E, et al. The macular choriocapillaris flow in glaucoma and within-day fluctuations: an optical coherence tomography angiography study. *Invest Ophthalmol Vis Sci*. 2021;62:22.
9. Demirtas AA, Karahan M, Ava S, Cilem Han C, Keklikci U. Evaluation of diurnal fluctuation in parafoveal and peripapillary vascular density using optical coherence tomography angiography in patients with exfoliative glaucoma and primary open-angle glaucoma. *Curr Eye Res*. 2021;46:96–106.
10. Wang X, Chen J, Zhang S, et al. Diurnal fluctuations of macular vessel density in patients with primary open-angle glaucoma and healthy subjects. *Int Ophthalmol*. 2020;40:2257–2266.

11. Rommel F, Rothe M, Kurz M, Prasuhn M, Grisanti S, Ranjbar M. Evaluating diurnal variations in retinal perfusion using optical coherence tomography angiography. *Int J Retina Vitreous*. 2020;6:22.
12. Milani P, Bochicchio S, Urbini LE, et al. Diurnal measurements of macular thickness and vessel density on OCT angiography in healthy eyes and those with ocular hypertension and glaucoma. *J Glaucoma*. 2020;29:918–925.
13. Lin E, Ke M, Tan B, et al. Are choriocapillaris flow void features robust to diurnal variations? A swept-source optical coherence tomography angiography (OCTA) study. *Sci Rep*. 2020;10:1–9.
14. Baek SU, Kim YK, Ha A, et al. Diurnal change of retinal vessel density and mean ocular perfusion pressure in patients with open-angle glaucoma. *PLoS One*. 2019;14(4):e0215684.
15. Yanik Odabas O, Demirel S, Ozmert E, Batioglu F. Repeatability of automated vessel density and superficial and deep foveal avascular zone area measurements using optical coherence tomography angiography: diurnal findings. *Retina*. 2018;38:1238–1245.
16. Burfield HJ, Carkeet A, Ostrin LA. Ocular and systemic diurnal rhythms in emmetropic and myopic adults. *Invest Ophthalmol Vis Sci*. 2019;60:2237–2247.
17. Burfield HJ, Patel NB, Ostrin LA. Ocular biometric diurnal rhythms in emmetropic and myopic adults. *Invest Ophthalmol Vis Sci*. 2018;59(12):5176–5187.
18. Read SA, Collins MJ, Iskander DR. Diurnal variation of axial length, intraocular pressure, and anterior eye biometrics. *Invest Ophthalmol Vis Sci*. 2008;49:2911–8.
19. Sindrup JH, Kastrop J, Christensen H, Jorgensen B. Nocturnal variations in peripheral blood flow, systemic blood pressure, and heart rate in humans. *Am J Physiol*. 1991;261(4 Pt 2):H982–H8.
20. Panza JA, Epstein SE, Quyyumi AA. Circadian variation in vascular tone and its relation to alpha-sympathetic vasoconstrictor activity. *N Engl J Med*. 1991;325:986–90.
21. Fernandez-Vigo JI, Kudsieh B, Shi H, et al. Normative database and determinants of macular vessel density measured by optical coherence tomography angiography. *Clin Exp Ophthalmol*. 2020;48:44–52.
22. Zhou Y, Zhou M, Gao M, Liu H, Sun X. Factors affecting the foveal avascular zone area in healthy eyes among young Chinese adults. *Biomed Res Int*. 2020;2020:7361492.
23. Brucher VC, Storp JJ, Eter N, Alnawaiseh M. Optical coherence tomography angiography-derived flow density: a review of the influencing factors. *Graefes Arch Clin Exp Ophthalmol*. 2020;258:701–710.
24. Harris A, Guidoboni G, Siesky B, et al. Ocular blood flow as a clinical observation: Value, limitations and data analysis [published online ahead of print January 24, 2020]. *Prog Retin Eye Res*, doi:10.1016/j.preteyeres.2020.100841.
25. Werne A, Harris A, Moore D, BenZion I, Siesky B. The circadian variations in systemic blood pressure, ocular perfusion pressure, and ocular blood flow: risk factors for glaucoma? *Surv Ophthalmol*. 2008;53:559–67.
26. Xiuyan Z, Qingmei T, Qiuxin W, et al. Thickness, vessel density of retina and choroid on OCTA in young adults (18–24 years old). *Microvasc Res*. 2021;136:104169.
27. Wang T, Li H, Zhang R, Yu Y, Xiao X, Wu C. Evaluation of retinal vascular density and related factors in youth myopia without maculopathy using OCTA. *Sci Rep*. 2021;11(1):15361.
28. Li S, Yang X, Li M, et al. The developmental changes of retinal microvasculature in children: a quantitative analysis using OCT angiography. *Am J Ophthalmol*. 2020;219:231–239.
29. Milani P, Montesano G, Rossetti L, Bergamini F, Pece A. Vessel density, retinal thickness, and choriocapillaris vascular flow in myopic eyes on OCT angiography. *Graefes Arch Clin Exp Ophthalmol*. 2018;256:1419–1427.
30. Leng Y, Tam EK, Falavarjani KG, Tsui I. Effect of age and myopia on retinal microvasculature. *Ophthalmic Surg Lasers Imaging Retina*. 2018;49:925–931.
31. Borrelli E, Lonngi M, Balasubramanian S, et al. Macular microvascular networks in healthy pediatric subjects. *Retina*. 2019;39:1216–1224.
32. Mo J, Duan A, Chan S, Wang X, Wei W. Vascular flow density in pathological myopia: an optical coherence tomography angiography study. *BMJ Open*. 2017;7(2):e013571.
33. Al-Sheikh M, Phasukkijwatana N, Dolz-Marco R, et al. Quantitative OCT angiography of the retinal microvasculature and the choriocapillaris in myopic eyes. *Invest Ophthalmol Vis Sci*. 2017;58:2063–2069.
34. Li M, Yang Y, Jiang H, et al. Retinal microvascular network and microcirculation assessments in high myopia. *Am J Ophthalmol*. 2017;174:56–67.
35. Liu M, Wang P, Hu X, Zhu C, Yuan Y, Ke B. Myopia-related stepwise and quadrant retinal microvascular alteration and its correlation with axial length. *Eye (Lond)*. 2020;35:2196–2205.
36. Su L, Ji YS, Tong N, et al. Quantitative assessment of the retinal microvasculature and choriocapillaris in myopic patients using swept-source optical coherence tomography angiography. *Graefes Arch Clin Exp Ophthalmol*. 2020;258:1173–1180.
37. Park SH, Cho H, Hwang SJ, et al. Changes in the retinal microvasculature measured using optical coherence tomography angiography according to age. *J Clin Med*. 2020;9:883.
38. You QS, Chan JCH, Ng ALK, et al. Macular vessel density measured with optical coherence tomography angiography and its associations in a large population-based study. *Invest Ophthalmol Vis Sci*. 2019;60:4830–4837.
39. Andrade Romo JS, Linderman RE, Pinhas A, Carroll J, Rosen RB, Chui TYP. Novel development of parafoveal capillary density deviation mapping using an age-group and eccentricity matched normative OCT angiography database. *Transl Vis Sci Technol*. 2019;8(3):1.
40. Wei Y, Jiang H, Shi Y, et al. Age-related alterations in the retinal microvasculature, microcirculation, and microstructure. *Invest Ophthalmol Vis Sci*. 2017;58:3804–3817.
41. Iafe NA, Phasukkijwatana N, Chen X, Sarraf D. Retinal capillary density and foveal avascular zone area are age-dependent: quantitative analysis using optical coherence tomography angiography. *Invest Ophthalmol Vis Sci*. 2016;57:5780–5787.
42. Yu J, Jiang C, Wang X, et al. Macular perfusion in healthy Chinese: an optical coherence tomography angiogram study. *Invest Ophthalmol Vis Sci*. 2015;56:3212–7.
43. Pilz LK, Keller LK, Lenssen D, Roenneberg T. Time to rethink sleep quality: PSQI scores reflect sleep quality on workdays. *Sleep*. 2018;41(5)
44. Flitcroft DI, He M, Jonas JB, et al. IMI—defining and classifying myopia: a proposed set of standards for clinical and epidemiologic studies. *Invest Ophthalmol Vis Sci*. 2019;60(3):M20–M30.
45. Czeisler CA, Waterhouse J. The effect of light on the human circadian pacemaker. *Ciba Found Symp*. 1995;183:254–290.
46. Fenner BJ, Tan GSW, Tan ACS, Yeo IYS, Wong TY, Cheung GCM. Identification of imaging features that determine quality and repeatability of retinal capillary plexus density measurements in OCT angiography. *Br J Ophthalmol*. 2018;102:509–514.

47. Lim HB, Kim YW, Kim JM, Jo YJ, Kim JY. The importance of signal strength in quantitative assessment of retinal vessel density using optical coherence tomography angiography. *Sci Rep.* 2018;8(1):12897.
48. Kraker JA, Omoba BS, Cava JA, et al. Assessing the influence of OCT-A device and scan size on retinal vascular metrics. *Transl Vis Sci Technol.* 2020;9(11):7.
49. Rabiolo A, Gelormini F, Marchese A, et al. Macular perfusion parameters in different angiocube sizes: does the size matter in quantitative optical coherence tomography angiography? *Invest Ophthalmol Vis Sci.* 2018;59:231–237.
50. Dong J, Jia YD, Wu Q, et al. Interchangeability and reliability of macular perfusion parameter measurements using optical coherence tomography angiography. *Br J Ophthalmol.* 2017;101(11):1542–1549.
51. Lal B, Alonso-Caneiro D, Read SA, Carkeet A. Induced refractive error changes the optical coherence tomography angiography transverse magnification and vascular indices. *Am J Ophthalmol.* 2021;229:230–241.
52. Chu Z, Lin J, Gao C, et al. Quantitative assessment of the retinal microvasculature using optical coherence tomography angiography. *J Biomed Opt.* 2016;21(6):66008.
53. Chiu SJ, Li XT, Nicholas P, Toth CA, Izatt JA, Farsiu S. Automatic segmentation of seven retinal layers in SDOCT images congruent with expert manual segmentation. *Opt Express.* 2010;18:19413–19428.
54. White WB. Systolic versus diastolic blood pressure versus pulse pressure. *Curr Cardiol Rep.* 2002;4:463–7.
55. Van Keer K, Breda JB, Pinto LA, Stalmans I, Vandewalle E. Estimating mean ocular perfusion pressure using mean arterial pressure and intraocular pressure. *Invest Ophthalmol Vis Sci.* 2016;57:2260.
56. Batschelet E. Circular statistics in biology. New York: Academic Press. 1981;388:1981;
57. Ostrin LA, Jnawali A, Carkeet A, Patel NB. Twenty-four hour ocular and systemic diurnal rhythms in children. *Ophthalmic Physiol Opt.* 2019;39:358–369.
58. Landler L, Ruxton GD, Malkemper EP. Grouped circular data in biology: advice for effectively implementing statistical procedures. *Behav Ecol Sociobiol.* 2020;74(8):100.
59. Landler L, Ruxton GD, Malkemper EP. Circular data in biology: advice for effectively implementing statistical procedures. *Behav Ecol Sociobiol.* 2018;72(8):128.
60. Pemp B, Georgopoulos M, Vass C, et al. Diurnal fluctuation of ocular blood flow parameters in patients with primary open-angle glaucoma and healthy subjects. *Br J Ophthalmol.* 2009;93:486–91.
61. Nesper PL, Lee HE, Fayed AE, Schwartz GW, Yu F, Fawzi AA. Hemodynamic response of the three macular capillary plexuses in dark adaptation and flicker stimulation using optical coherence tomography angiography. *Invest Ophthalmol Vis Sci.* 2019;60:694–703.
62. Samara WA, Say EAT, Khoo CTL, et al. Correlation of foveal avascular zone size with foveal morphology in normal eyes using optical coherence tomography angiography. *Retina.* 2015;35:2188–2195.
63. Savastano MC, Lumbroso B, Rispoli M. In vivo characterization of retinal vascularization morphology using optical coherence tomography angiography. *Retina.* 2015;35:2196–203.
64. Falavarjani KG, Shenazandi H, Naseri D, et al. Foveal avascular zone and vessel density in healthy subjects: an optical coherence tomography angiography study. *J Ophthalmic Vis Res.* 2018;13:260–265.
65. Lavia C, Couturier A, Erginay A, Dupas B, Tadayoni R, Gaudric A. Reduced vessel density in the superficial and deep plexuses in diabetic retinopathy is associated with structural changes in corresponding retinal layers. *PLoS One.* 2019;14(7):e0219164.
66. Chen W, Lou J, Thorn F, et al. Retinal microvasculature in amblyopic children and the quantitative relationship between retinal perfusion and thickness. *Invest Ophthalmol Vis Sci.* 2019;60:1185–1191.
67. Kern TS. Do photoreceptor cells cause the development of retinal vascular disease? *Vis Res.* 2017;139:65–71.
68. Guido ME, Garbarino-Pico E, Contin MA, et al. Inner retinal circadian clocks and non-visual photoreceptors: novel players in the circadian system. *Prog Neurobiol.* 2010;92:484–504.
69. Huemer KH, Zawinka C, Garhofer G, et al. Effects of dopamine on retinal and choroidal blood flow parameters in humans. *Br J Ophthalmol.* 2007;91:1194–8.
70. Doyle SE, McIvor WE, Menaker M. Circadian rhythmicity in dopamine content of mammalian retina: role of the photoreceptors. *J Neurochem.* 2002;83:211–9.
71. Yu J, Gu R, Zong Y, et al. Relationship between retinal perfusion and retinal thickness in healthy subjects: an optical coherence tomography angiography study. *Invest Ophthalmol Vis Sci.* 2016;57(9):OCT204–10.
72. Portaluppi F, Tiseo R, Smolensky MH, Hermida RC, Ayala DE, Fabbian F. Circadian rhythms and cardiovascular health. *Sleep Med Rev.* 2012;16:151–66.
73. Muller VC, Storp JJ, Kerschke L, Nelis P, Eter N, Alnawaiseh M. Diurnal variations in flow density measured using optical coherence tomography angiography and the impact of heart rate, mean arterial pressure and intraocular pressure on flow density in primary open-angle glaucoma patients. *Acta Ophthalmol.* 2019;97(6):e844–e849.
74. Ott C, Raff U, Harazny JM, Michelson G, Schmieder RE. Central pulse pressure is an independent determinant of vascular remodeling in the retinal circulation. *Hypertension.* 2013;61:1340–5.
75. Singleton CD, Robertson D, Byrne DW, Joos KM. Effect of posture on blood and intraocular pressures in multiple system atrophy, pure autonomic failure, and baroreflex failure. *Circulation.* 2003;108:2349–54.
76. Tell GS, Prineas RJ, Gomez-Marin O. Postural changes in blood pressure and pulse rate among black adolescents and white adolescents: the Minneapolis Children's Blood Pressure Study. *Am J Epidemiol.* 1988;128:360–369.
77. Munsamy AJ, Gopaul K, Perumal K, et al. A comparative analysis of the postural and diurnal ocular perfusion pressure of young healthy individuals of different ethnicities. *African Vis Eye Health.* 2018;77(1):1–8.
78. Eşer İ, Khorshid L, Yapucu Güneş Ü, Demir Y. The effect of different body positions on blood pressure. *J Clin Nurs.* 2007;16:137–140.
79. Feke GT, Pasquale LR. Retinal blood flow response to posture change in glaucoma patients compared with healthy subjects. *Ophthalmology.* 2008;115:246–52.
80. Lam AKC, Wong S, Lam CSY, To CH. The effect of myopic axial elongation and posture on the pulsatile ocular blood flow in young normal subjects. *Optom Vis Sci.* 2002;79:300–305.
81. Kothe AC. The effect of posture on intraocular pressure and pulsatile ocular blood flow in normal and glaucomatous eyes. *Surv Ophthalmol.* 1994;38(Suppl):S191–7.
82. Liu X, Shen M, Yuan Y, et al. Macular thickness profiles of intraretinal layers in myopia evaluated by ultrahigh-resolution optical coherence tomography. *Am J Ophthalmol.* 2015;160:53–61.e2.
83. Zhu Q, Xing X, Wang M, et al. Characterization of the three distinct retinal capillary plexuses using optical coherence tomography angiography in myopic eyes. *Transl Vis Sci Technol.* 2020;9(4):8.

84. Patton N, Maini R, MacGillivray T, Aslam TM, Deary IJ, Dhillon B. Effect of axial length on retinal vascular network geometry. *Am J Ophthalmol*. 2005;140:648–53.
85. Lam AK, Chan ST, Chan B, Chan H. The effect of axial length on ocular blood flow assessment in anisometropes. *Ophthalmol Physiol Opt*. 2003;23:315–20.
86. Benavente-Perez A, Hosking SL, Logan NS, Broadway DC. Ocular blood flow measurements in healthy human myopic eyes. *Graefes Arch Clin Exp Ophthalmol*. 2010;248:1587–94.
87. Kur J, Newman EA, Chan-Ling T. Cellular and physiological mechanisms underlying blood flow regulation in the retina and choroid in health and disease. *Prog Retin Eye Res*. 2012;31:377–406.
88. Tamaki M, Bang JW, Watanabe T, Sasaki Y. Night watch in one brain hemisphere during sleep associated with the first-night effect in humans. *Curr Biol*. 2016;26:1190–4.
89. Ehrlich R, Kheradiya NS, Winston DM, Moore DB, Wirostko B, Harris A. Age-related ocular vascular changes. *Graefes Arch Clin Exp Ophthalmol*. 2009;247:583–91.
90. Norton TT, Siegwart JT, Jr. Light levels, refractive development, and myopia—a speculative review. *Exp Eye Res*. 2013;114:48–57.